IEEE Access
Multidisciplinary | Rapid Review | Open Access Journal

Received February 11, 2020, accepted March 3, 2020, date of publication March 9, 2020, date of current version March 25, 2020.

Digital Object Identifier 10.1109/ACCESS.2020.2979326

Simultaneous Enhancement of Scanning Area and Imaging Speed for a MEMS Mirror Based High Resolution LiDAR

PALLAB K. CHOUDHURY[1,2,3], (Member, IEEE), AND CHANG-HEE LEE[1,2], (Fellow, IEEE)

[1]Liangjiang International College, Chongqing University of Technology, Chongqing 401135, China
[2]Department of Electrical Engineering, Korea Advanced Institute of Science and Technology (KAIST), Daejeon 34141, South Korea
[3]Department of Electronics and Communication Engineering, Khulna University of Engineering & Technology (KUET), Khulna 9203, Bangladesh

Corresponding author: Chang-Hee Lee (changheelee@kaist.ac.kr)

This work was supported in part by the Project under Grant WQ20165000357 of Chinese Government.

ABSTRACT High speed imaging with improved resolution and wide area scanning are the ultimate targets for designing a MEMS mirror based LiDAR. Simultaneous improvements of above parameters are critical and yet pose design tradeoff among system complexity, cost and compatibility. Here, we propose a high resolution LiDAR for wide area scanning with improved frame rate by allowing minimum design constrains. Extended area scanning is achieved by simplified transmitter design with off-the-shelf low cost optics such as a beam splitter cube and a plane mirror. In addition, an effective scanning strategy is applied to improve the imaging speed for the extended coverage area, which involves sub-pixel imaging of selectively and sequentially shined target areas. Then, a high resolution image can be reconstructed after merging all the sub-pixel values. The proposed architecture is experimentally demonstrated to reconstruct a high resolution image of 1020 × 500 pixels at the fast refresh rate of 20 *fps* in extended FoV 52° × 26°. The system is also characterized in terms of linearity of extended optical angles, intensity distribution of light beam profile at several angular positions, and quality of scanned objects in the high resolution reconstructed image.

INDEX TERMS Light detection and ranging (LiDAR), optical imaging, microelectromechanical-system (MEMS), laser scanning, image reconstruction.

I. INTRODUCTION

It is always interesting to see our surrounding in 3D view with enough resolution. Sensors typically play an important role to build such multi-dimensional scenario by acquiring different attributes of the target objects. In the field of active optical imaging, a target is illuminated by a light source and thus, it can effectively improve the image resolution by simultaneous acquisition of depth and spatial information. A light detection and ranging (LiDAR) is a key sensor for this 3D optical imaging technology [1]–[3]. In recent years, LiDAR shows enormous potential in different applications including geographic information system, robotics, medical diagnostics, computational imaging and driving an autonomous vehicle [4]–[8]. To obtain high resolution image with improved signal-to-noise ratio (SNR), LiDAR needs to employ a laser scanning module with sufficient Field-of-View (FoV) covering large number of scanning steps. In each angular scanning position, the target was exposed and the reflected light was detected to extract spatial and depth information for 3D image formation. Therefore, the performance of such LiDAR mostly depends on the selection of proper scanning components (e.g., a MEMS, a scanning mirror, a galvanometer scanner, the Risley prism pair and so on). Among them, the MEMS mirror has been used in several LiDARs due to its small size, fast speed, low power consumption etc. [9]–[11]. However, the MEMS mirror based scanning LiDAR suffers from two main limitations; a *small scanning angle* of MEMS mirror itself, *slow imaging speed/frame rate* as introduced by point-to-point scanning for the development of *high resolution* wide view image.

The mechanical tilt angle of a MEMS mirror is often less than 7°, which is again depends on the actuator types (integrated and bonded) and driving modes (quasi-static and resonant). Moreover, there are also design tradeoff between a scanning speed, a mirror size and a tilt angle. The MEMS tilt angle reduces with increase of the scanning speed and the mirror size, and vice versa. Recently, several investigations have

The associate editor coordinating the review of this manuscript and approving it for publication was Md. Moinul Hossain.

This work is licensed under a Creative Commons Attribution 4.0 License. For more information, see https://creativecommons.org/licenses/by/4.0/

focused on the widening of the scanning angle of the MEMS mirror and thus, proposed number of methods including fabrication of new MEMS structure as well as innovative system design [12]–[18]. Electromagnetic [12] and piezoelectric [13] actuators were used to design a quasi-static MEMS mirror, however, the scan angle was not large enough for designing a wide scanning LiDAR. Multiple laser diodes (LDs) and associate lens were also utilized to cover the scanning angle of 45° [14]. However, the propose system significantly increases the design complexity due the control of several LDs with relevant driving circuits and also, adjustment of individual/mutual lens position to ensure optimum focus on the MEMS mirror. Beside this, customized lenses are used for optical angle amplification such as fisheye lens [15], telescope-type lens [16], [17], f-theta lens [18]. Three spherical lenses are used in [15], which eventually introduces f-theta distortion in optical amplification at a large scanning angle. Moreover, nonlinearity arises among the scanning angles due to the placement of positive and negative lens in either side of a MEMS mirror. To maintain the linear operation, f-theta lenses are used in [18], however, it again increases the cost and design complexity due to the presence of too many lenses.

Beside the optical scanning angle, the image frame rate and resolution are also crucial performance parameters for the MEMS based LiDAR. A LiDAR needs to maintain an image frame rate as high as possible, in particular, it should be above 15 *fps* for applications like high speed vehicle navigation [1]. Moreover, maintaining a good frame rate again relate with image resolution. Usually, a high resolution image relies on the high-resolution scanning angles and thus, a large number of scanning steps are required for the MEMS module. However, this requirement increases the scanning time, which reduces the imaging speed or the frame rate. Both these design parameters become more critical when the LiDAR scanning angle is wide. Hence, it is necessary to consider both scanning angle and imaging seed to design a high resolution MEMS based LiDAR. A non-scanning LiDAR (*Flash* LiDAR) can improve the imaging speed, however, it suffers from low SNR. To reach the required level of SNR with high resolution image, the flash LiDAR typically uses large size focal plane array receiver with high sensitive single photon avalanche diodes [19], [20]. However, developing of such kind of receiver array is technically challenging and very costly.

Overall, there are still couple of common issues that are not highlighted in previous investigations [12]–[18], however, they have significant impact on the efficient design of MEMS based LiDAR. *Firstly,* most of the above works utilize the customized single/multiple lens structure, where the performance validation is mainly based on analytical or numerical simulation results. Due to the lack of sufficient experimental details using those customized components, the proposed solutions are limited in availability and introduce compatibility issue to use in already deployed LiDAR. *Secondly,* nonlinearity in scanning angles is addressed by several ways, however, its effect is still present especially for large MEMS tilt angel $> 4°$. The divergence of beam is significantly increased at wide view angles of a MEMS mirror. *Finally,* the earlier methods of wide scanning angle were not tested to evaluate the system performance for high speed imaging with improved resolution.

Here, we propose and experimentally demonstrate a MEMS mirror based wide angle scanning method for simultaneous improvement of imaging speed and viewing angle by applying reduce number of scanning steps for a high resolution LiDAR with simplified transmitter design. Overall, the main contributions of this paper can be summarized as follows:

a) *Extended scanning angle* $52° \times 26°$ is experimentally demonstrated by using low cost optics such as an optical beam splitter cube and a plane mirror. Both components are available commercially in different sizes and most importantly, they have the good performance to maintain linear relation between incident and output optical transmission. The proposed design is also quite compatible for a commercial LiDAR to improve the MEMS scanning angles with minimum changes in hardware.

b) *Fast frame rate* is achieved by introducing a scanning strategy, where the number of scanning steps of MEMS mirror are significantly reduced even to cover a wide FoV. Instead of point-by-point scanning, a selective area of target is imaged at every MEMS tilt angle and the corresponding reflected images are detected by a sensor array. Moreover, the extended scanning portion is covered by the beam spots, which are the replica of original spots and thus, both the imaging areas (original + extended) are scanned by two sub-pixel spots operated at a time. This strategy again accelerates the scanning operation to reach in high frame rate. The effectiveness of the propose technique is evaluated by experiment to reach the fast frame rate upto 20 *fps*in extended FoV $52° \times 26°$.

c) *High resolution image* is re-constructed by merging all the received values of each sub-pixel sensor array, which is shined during the selective scanning. A selective laser scanning with small imaged area ensures high SNR in compare to whole area scan by using flash light. A sub-pixel array size of 50×50 is utilized for each scanning step, which is sequentially collected and synchronized to form a high resolution image of 1020×500 pixels with improved SNR performance. Objects are clearly marked in the good quality image with adequate details of shape and reflectivity information.

The rest of the paper is organized as follows, section II presents the propose model of the MEMS mirror based scanning LiDAR and discuss its experimental setup. Section III shows the performance results of extended optical angles and also, characterizes the laser beam profiles. Sections IV discuss details on the process of high resolution image reconstruction including the relevant imaged spots at multiple scanning positions. Finally, key results of this paper with future path of improvement are discussed as conclusion in section V.

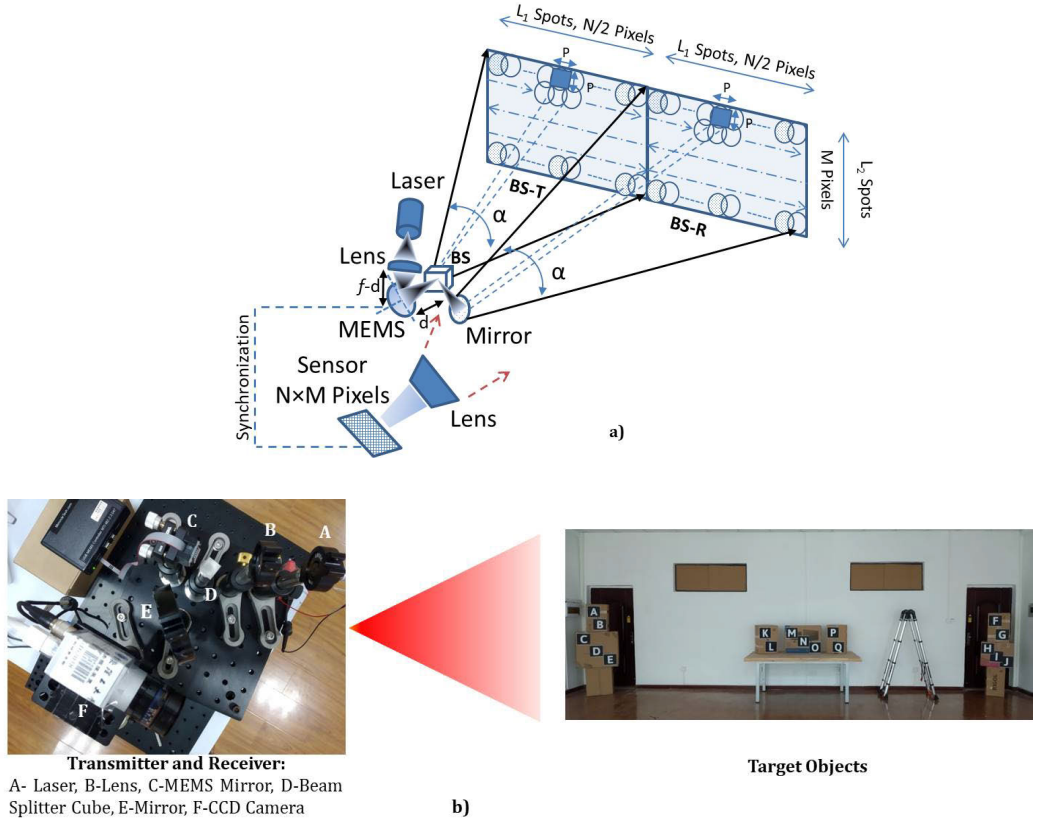

FIGURE 1. a) Propose MEMS mirror based wide angle high resolution scanning LiDAR b) Experimental Setup and target objects to reconstruct image.

II. PROPOSE MEMS BASED SCANNING LiDAR AND EXPERIMENTAL SETUP

The design principle of a MEMS mirror based scanning LiDAR and its experimental setup is shown in Fig. 1. A commercially available dual-axis MEMS mirror (Mirrocle Tech., 3.6 mm diameter, maximum mechanical tilt angle $\geq \pm 6.55°$ in quasi-static mode) is used in transmitter side, where the incident light is collimated by a lens (plano convex) followed by a 635 nm RED laser with 10 mW average optical emission power. MEMS mirror size needs to be selected based on the input laser beam quality/shape that can be confined properly on the surface of mirror for the efficient reflection, however for the propose methods, there is no such direct impact of MEMS mirror size on the claimed advantages. The driving voltages of MEMS mirror is adjusted to set the optical scanning angle of $26° \times 26°$ (α) so that the extended scanning angle ($\sim 2\alpha$) can finally matched with receiver FoV of $52° \times 26°$. The reflected light from a MEMS mirror is then divided into two parts by using an optical beam splitter (BS) cube (split ratio: 50/50, 10mm $\times$ 10mm $\times$ 10mm). One part transmits along the axis of incident light beam (BS-T), whereas, the other part will be reflected by a plane mirror (BS-R). Finally, both the light beams (BS-T and BS-R) transmit toward the direction of object to shine different sections of the target image. By adjusting the positions of the beam splitter and the plane mirror, two scanning beams can effectively cover the wide target area close to twice of original scanning angle as covered by a single MEMS mirror.

Moreover, the propose system also develops an effective scanning strategy to work with extended scanning operation, which will ensure a simultaneous improvement of both the optical scanning angle and the imaging speed to reconstruct the target image. In this approach, the incoming laser beam is shaped such that the number of scanning steps can be reduced to cover the whole target area, which eventually improves the imaging speed. In the experiment, only 10×8 ($L_1 \times L_2$) spots are used to cover scanning angle of $26° \times 26°$ (α) in one side, whereas the other part of the target area is a replica as produced by plane mirror reflection. Therefore, the full scanning area is now extended to $52° \times 26°$ with two spots at a time for every scanning step of the MEMS mirror. Note that this improvement of scanning angle is achieved with the same scanning time of the MEMS mirror as originally set for the angle $26° \times 26°$. In addition, a scanning pattern is designed such that the circular shaped adjacent spots are partially overlapped to reduce the inter-circular gap, where the effective pixel size is $P \times P$ as shown in fig. 1(a).

The targets are placed at a 10-meter distance from transmitter/receiver side, which consist of multiple objects with different reflective surfaces and color including box cartons with English alphabet (color of Gray/Black/White), laboratory table, portable steel stair and white wall. The objects

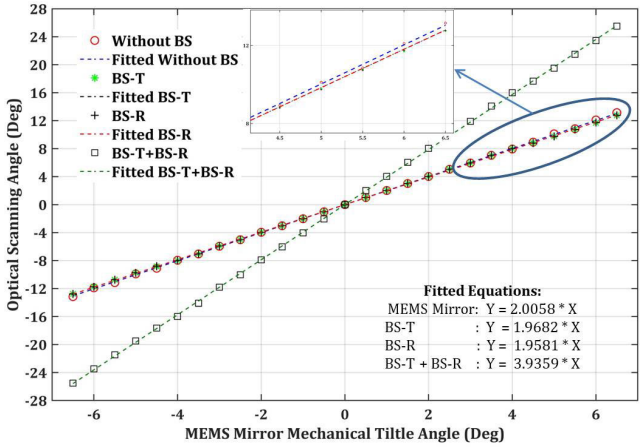

FIGURE 2. Optical scanning angles in terms of MEMS tilt angles.

are placed in distributed way to cover the extended scanning angle of 52° ×26° as imaged by laser scanning and focused by the receiver lens. At a time, two shined spots are imaged in the receiver sensor array with the corresponding pixel values of target reflectivity. The pixel values from all the imaged spots are merged to reconstruct the high resolution target image. In the experiment, a CCD camera of 1020 × 500 ($N \times M$) resolution and a wide angle lens (4 mm focal length) are used in the receiver side to retrieve the pixel information of all the imaged spots. The horizontal FoV of the receiver (1/3″ sensor, 4 mm lens) is 52.5°, which is well matched for extended scanning angle of 52°. It may be noted that CCD camera based LiDAR is extensively investigated recently for 3D imaging due to its mature technology, high resolution pixels and low cost optical receiver [21], [22]. Moreover, the above transmitter-receiver distance is maintained based on the transmitted optical power and sensitivity of optical receiver, however, necessary adjustments are needed for long distance operation either in transmitter side, by placing a high power laser source or in receiver side, by using a highly sensitive CCD sensor or APD array. Finally, pixel processing, merging of pixel data, synchronization, and reconstruction of the target image were done by a computer.

III. EVALUATION OF EXTENDED OPTICAL SCANNING ANGLE

A. SLOP OF OPTICAL SCANNING ANGLES

The proposed system performance is analyzed for the extended scanning angle operation and the results are shown in Fig. 2. Figure 2 shows the experimentally measured values of optical scanning angles with respect to MEMS mechanical tilt angles. Each of the measured values are fitted by an equation $y = a.x + b$, where a indicates the slop of the fitted line and b provides a constant value. As $a \gg b$, the values of b are excluded from the final fitted linear equations. As expected, the optical tilt angle by the MEMS mirror (without BS and plane mirror) is two time that of the mechanical tilt angle. The measured values and fitted line with slope a of 2.00058 clearly justify this relation of mechanical tilt vs optical tilt angles of the MEMS mirror. With the addition of the BS and the plane mirror, two beams (BS-T and BS-R) are generated with relevant scanning angles that eventually cover the whole target area. The individual contribution of optical scanning angles for both beams are separately measured and fitted with two lines. It should be noted that the optical beam should be maintained its shape within whole optical amplification angle. Thus the incident angle and size of the BS should be designed to ensure this.

Figure 2 shows that the slopes of the fitted lines are 1.96 and 1.95 corresponding to the BS-T and the BS-R beams. These values are close enough to the original scanning slop of $a = 2.0058$ for the MEMS mirror operates alone. The slight degradation in the slop values are mainly appeared from the size of the BS itself, which is not optimum especially for a large mechanical tilt angle of the MEMS mirror. In particular, the incident beams are not properly confined to the BS for the MEMS mechanical tilt angle of larger than 4.5°. A properly design BS cube that match with incident scanning angles are useful to overcome this loss. Finally, both the BS-T and the BS-R optical scanning angles are combined to measure the full extended FoV for the proposed system as also shown in Fig. 2. The slope value of the fitted line is measured to 3.968, which indicates around four-fold improvement of optical scanning angles in compare to the MEMS mechanical tilt angle. Overall, the proposed technique shows good linearity in amplified scanning angles as produced by both BS-T and BS-R.

B. INTENSITY PROFILE OF BEAM

The intensity profile of beam is considered to be important performance parameter, since it determines the quality of scanning system. To qualify this, we measured the intensity profile of the beams as function of the scanning angle. These are compared with to the reference beam profile that was measured just after the MEMS mirror as shown in fig. 3(a). Note that in order to minimize the distortion of the beam over whole scanning range, distance between the lens to the MEMS mirror and the MEMS mirror to the beam splitter (BS) is crucial. Figure 1(a) shows that the distance from the MEMS mirror to the BS is maintained as d such that there is (f-d) distance from the MEMS mirror to the lens, where f is the focal length of the lens. By using this adjustment, the focal point of the lens is located on the BS. Then, we can minimize the distortion due to finite size of the BS. Figure 3(a) shows the beam spots in the extended optical scanning angles of −26°, −13°, +13°, +26°. Overall, the beam profiles do not show significant distortion in compare to the reference beam.

Finally, all the measured points are fitted with a high order Gaussian beam profile, which shows relatively flat top in maximum intensity and slow transition at the edge of the curve in fig. 3(b). All the curves almost coincide to each other, where the measured spot size is measured to around 40 cm @ 10 meters distance. However, there are some intensity irregularities, which are mostly come from laser itself (fig. 3(c)) due to the presence of side fringes. A good spatial filter or beam shaper can be used to make the beam spot more uniform.

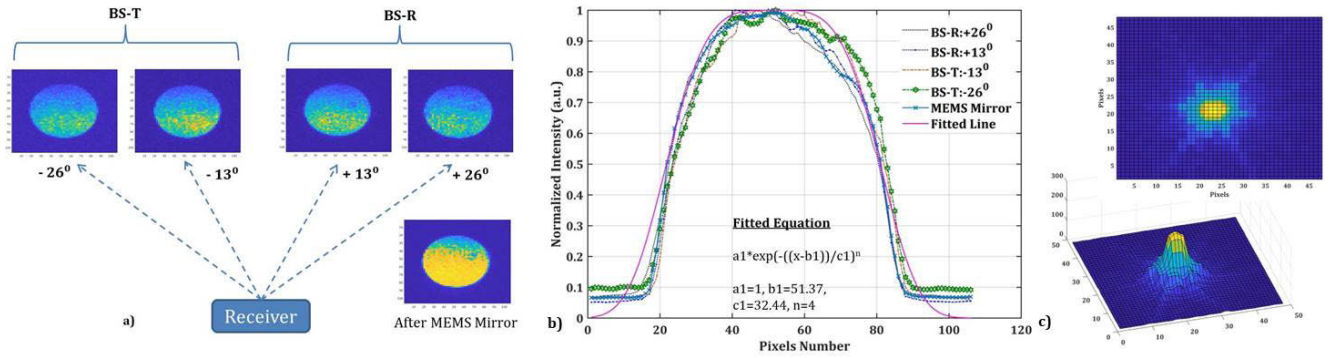

FIGURE 3. a) The measured beam shapes at different angles b) Beam profiles fitted with super Gaussian distribution c) Intensity distribution of Laser spot in 2D and 3D view.

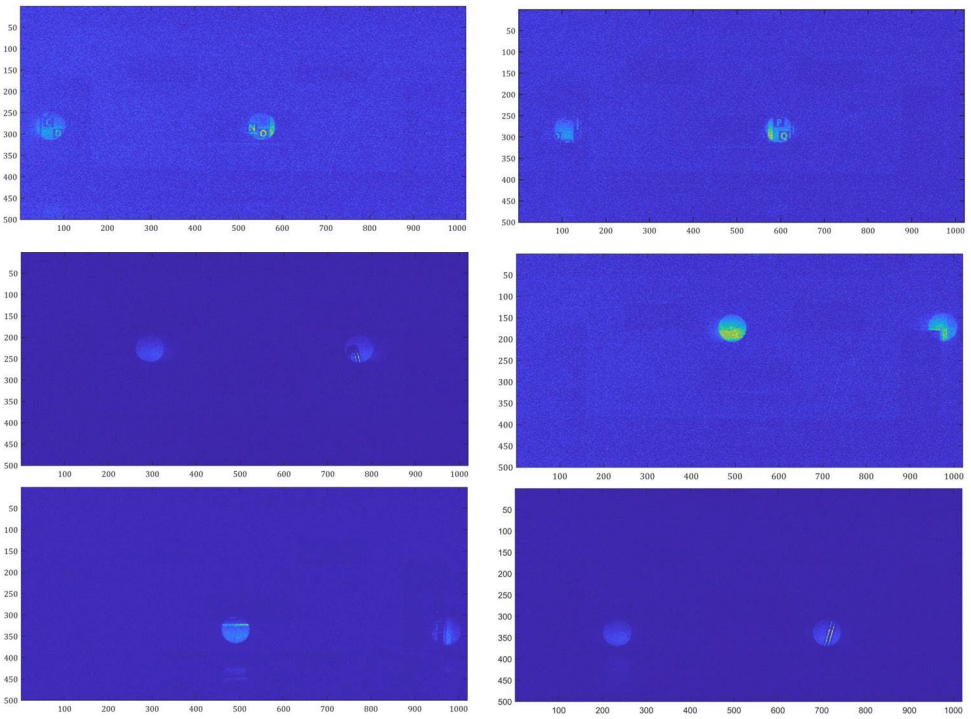

FIGURE 4. Randomly selected two imaged spots at different scanned positions of target objects.

Overall, the angular resolution/accuracy of the propose system depends on the scanning FoV and receiver pixel size. For the demonstrate system, the scanning FoV is 52° (H) × 26° (V) and receiver pixel size is 1020 (H) × 500 (V) and thus the angular resolution is (52/1020)≅ 0.05° in Horizontal and (26/500) ≅ 0.05° in vertical direction. As the scanned images of original scanning area (BS-T) and extended area (BS-R) are resolved into independent pixels with equal sizes at receiver side, the system angular resolution is maintained same even in the extended angle operation.

IV. PROCESS OF IMAGE RECONSTRUCTION

A. FAST IMAGING SPEED IN EXTENDED FoV

The proposed system for extended fov is further investigated to acquire an image, where the imaging speed is improved by introducing an effective scanning strategy as discussed before. The results of the target image acquisition and corresponding high resolution image reconstruction process are shown in fig.4 and fig. 5. As mention before, the target objects consist of different reflective materials including its color, size, and relevant order. The positions of the BS and the plane mirror are adjusted such that the emitted beams (BS-T and BS-R) can effectively cover the extended angles of the MEMS scanning i.e. 52° × 26°. The scanning pattern is created by the MEMS controller with 8 lines in vertical direction, where each line has 10 spots horizontally. Therefore, there are only 80 spots to cover the FoV of 26° × 26° in one side, which will be mirrored in the other part to fulfill the total extended scanning angles of 52° × 26°. The numbers of scanning spots are selected based on the effective coverage of whole object area by using circular shaped image region.

Note that this reduction of scanning steps gives the system boost to reach an adequate frame rate. Moreover, due to the arrival of two spots at a time, the same scanning time

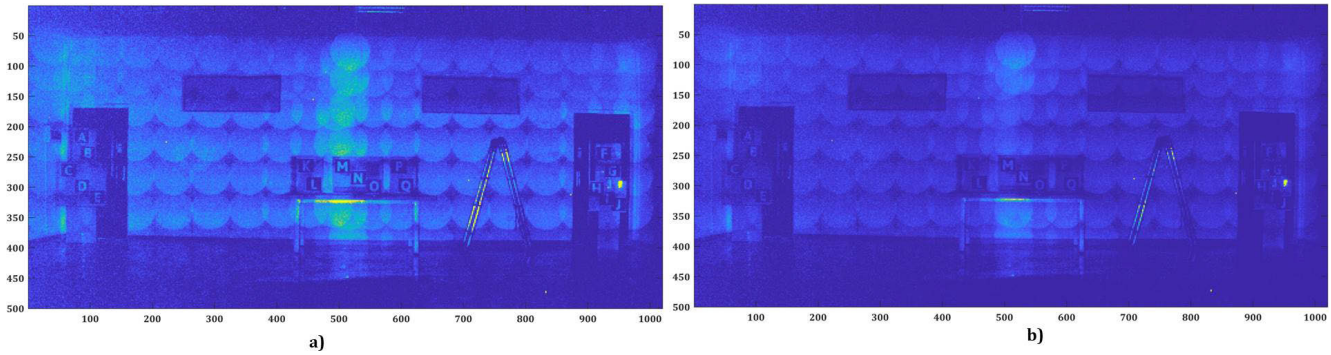

FIGURE 5. Re-constructed image after merging all the imaged spots at a) 15 *fps* and b) 20 *fps*.

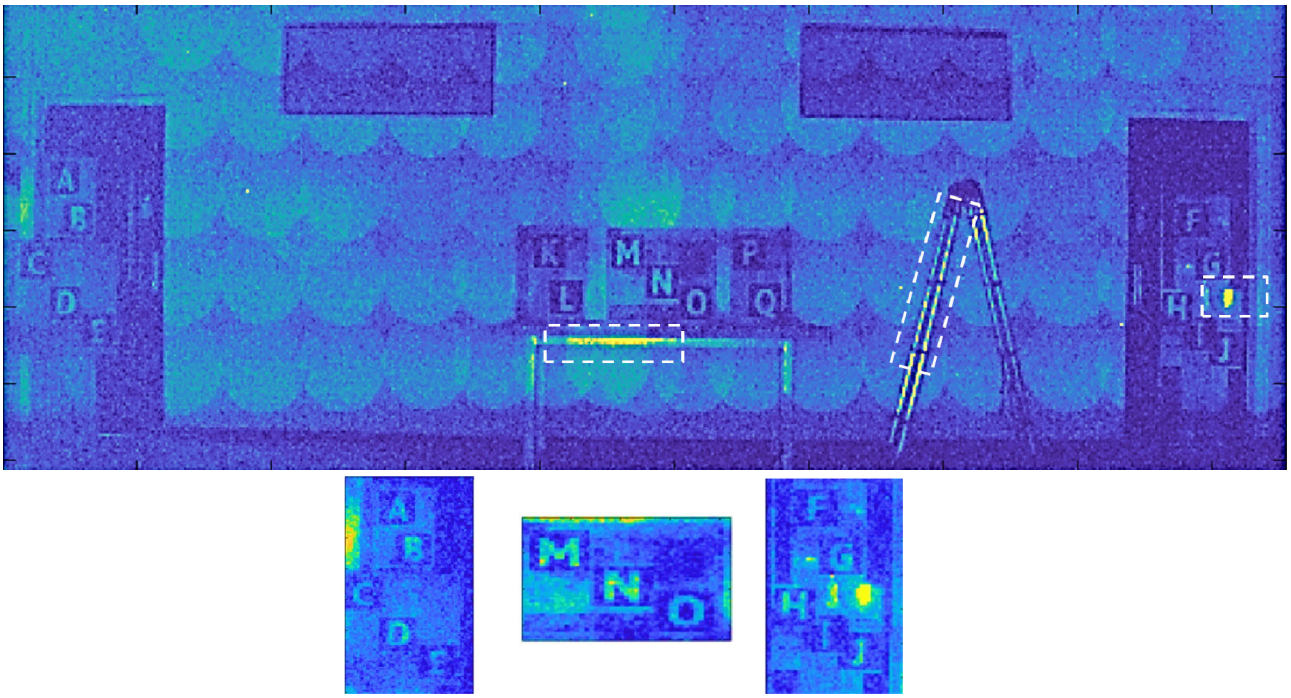

FIGURE 6. Processed image to enhance the visual quality of target objects; dotted box shows highly reflective object surfaces; Alphabet are zoomed separately (down figures).

as set for one part (26° × 26°) is still useful to cover the total area (52° × 26°), which gives an additional benefit to ensure high speed imaging. Above all, driving the MEMS mirror with a given scanning angle is now simple due to the reduced number of scanning steps (10/line). However, for a conventional LiDAR, this driving strategy is quite critical due to huge scanning steps for a high angular resolution.

In the experiment, the scanning time of each line is adjusted to ∼ 8.3 ms (frame time∼ 66.5 ms) and ∼ 6.3 ms (frame time ∼ 50 ms) for the imaging speed of 15 *fps* and 20 *fps* respectively. Finally, the MEMS controller scanning time is synchronized with camera acquisition time to ensure required frame rate for image reconstruction. For every scanning step, there are two shined spots that are imaged and corresponding pixel values are retrieved by the sensor as shown in fig.4. Figure 4 clearly shows that the two beam spots are scanned from two different parts of target image. The two spots are separated by the angle 26°, and rotate together in every horizontal/vertical scanning direction to cover the wide FoV region. After completion of full area scanning with required refresh rate, the corresponding pixel values of all the image spots are retrieved, synchronized and merged to reconstruct a high resolution scanned image as shown in fig. 5.

B. HIGH RESOLUTION SCANNED IMAGE

As mentioned before, high resolution LiDAR imaging by scanning or non-scanning (Flash) suffers from either low scanning rate, due to increase of scanning steps or low SNR, due to decrease of power density in large area. Here, the proposed method along with scanning strategy can effectively improve the imaging rate and SNR to re-construct the high resolution image. Instead of shine the whole target area with a single shot like in flash LiDAR, the propose scanning method shines a part of it that corresponds to a sub-pixel size of

sensor array. The sub-pixel size of image is useful for wide scanning to maintain fast frame rate due to the reduction of scanning steps and also, these can be utilized to re-construct the high resolution image by merging all the sub-pixel image values. Moreover, such scanning strategy ensures increase of power density in the selective area scan, which eventually improves the SNR of re-construct image. The approach shows the compromise between the improvement of SNR and scanning speed. For our experiment, the total target area was 31.4159 m^2, whereas the proposed selective scanning strategy uses only 0.1194 m^2 for each imaged area and thus, the power to the given area is improved by around 21.2 dB, considering that the scanning beam was slightly elliptical (n=4) with power difference for different scan positions was negligible.

In the experiment, the effective sub-pixel size of each image (fig.1) is close to 50 × 50 (P × P) and there are two images at a time in CCD sensors. After completion of single frame scanning, all the images are synchronized and merged together to form a high resolution image of 1020 × 500 corresponds to 52° ×26° as shown in fig. 5. Figure 5 shows the reconstructed image that provides a clear inside of scanned objects for both the refresh rate of 15 *fps* and 20 *fps*. With the increase of refresh rate from 15 *fps* to 20 *fps*, the overall image intensity is reduced due to the decrease of photon density per pixel.

The whole image is further processed to enhance its visual quality with the help of techniques like thresholding, contrast adjustment and the resultant image is shown in fig.6. Advanced image processing algorithms may also apply for further improvement of image quality [23], [24]; however, such studies are out of scope for the present work.

Based on reflectivity of target, image intensity changed and might show a high intensity from smooth surfaces like stainless steel and retro-reflector as indicated by dotted box in fig.6. The measured size of each alphabet is around 15 × 22 cm which is scanned from 10-meter distance and the corresponding processed image is highlighted separately in fig.6. The result shows that the reconstructed image quality is adequate to understand each of the details of target object. For developing a high resolution image with the presence of large size of CCD sensor at the receiver, the angular resolution still maintains the same value over the full scanning area as long as the scanned images are captured, retrieved and reconstructed from independently excited pixels as propose in this article.

V. CONCLUSION

A simplified transmitter and fast scanning strategy are introduced for design of a high resolution LiDAR based on a MEMS mirror. The proposed architecture is experimentally demonstrated to show three fold improvement; extended optical angles reach to 52° × 26° by simultaneous scanning of two imaged spots, high imaging rate upto 20 *fps* by using sub-pixel shined image with reduce number of scanning steps, and high resolution 1020 × 500 image reconstruction with the help of synchronous addition of all the sub-pixel (50 × 50) values. The presented results are useful to develop a low cost and high speed solid state LiDAR for diverse applications. Solid state LiDAR is considered to be good alternative for minimizing the limitations of conventional mechanical rotation based LiDAR due to its compact size, light weight and low power consumption. Further development of propose methods include the image quality enhancement with advance image processing algorithms as well as and mapping the object area with depth information for 3D view.

REFERENCES

[1] B. Schwarz, "LIDAR: Mapping the world in 3D," *Nature Photon.*, vol. 4, no. 7, pp. 429–430, 2010.

[2] P. F. McManamon, "Review of ladar: A historic, yet emerging, sensor technology with rich phenomenology," *Opt. Eng.*, vol. 51, no. 6, Jun. 2012, Art. no. 060901.

[3] Y. Cheng, J. Cao, F. Zhang, and Q. Hao, "Design and modeling of pulsed-laser three-dimensional imaging system inspired by compound and human hybrid eye," *Sci. Rep.*, vol. 8, no. 1, Dec. 2018, Art. no. 17164.

[4] V. Roback, A. Bulyshev, F. Amzajerdian, and R. Reisse, "Helicopter flight test of 3D imaging flash LIDAR technology for safe, autonomous, and precise planetary landing," *Proc. SPIE*, vol. 8731, pp. 1–20, Jun. 2013.

[5] D. F. Pierrottet, F. Amzajerdian, B. L. Meadows, R. Estes, and A. M. Noe, "Characterization of 3-D imaging lidar for hazard avoidance and autonomous landing on the moon," *Proc. SPIE*, vol. 6550, Apr. 2007, Art. no. 655008.

[6] C.-I. Chen and R. Stettner, "Drogue tracking using 3D flash lidar for autonomous aerial refueling," *Proc. SPIE*, vol. 8037, pp. 1–11, May 2011.

[7] B. Sun, M. P. Edgar, R. Bowman, L. E. Vittert, S. Welsh, A. Bowman, and M. J. Padgett, "3D computational imaging with single-pixel detectors," *Science*, vol. 340, no. 6134, pp. 844–847, May 2013.

[8] W. Gong, C. Zhao, H. Yu, M. Chen, W. Xu, and S. Han, "Three-dimensional ghost imaging lidar via sparsity constraint," *Sci. Rep.*, vol. 6, no. 1, Sep. 2016, Art. no. 26133.

[9] R. Moss, P. Yuan, X. Bai, E. Quesada, R. Sudharsanan, B. L. Stann, J. F. Dammann, M. M. Giza, and W. B. Lawler, "Low-cost compact MEMS scanning ladar system for robotic applications," *Proc. SPIE*, vol. 8379, May 2012, Art. no. 837903.

[10] Y. Takashima, B. Hellman, J. Rodriguez, G. Chen, B. Smith, A. Gin, A. Espinoza, P. Winkler, C. Perl, C. Luo, E. Kang, Y. Kim, H. Choi, and D. Kim, "MEMS-based imaging LIDAR," in *Proc. Opt. Photon. Energy Environ.*, 2018, pp. 1–2, Paper ET4A.1.

[11] H. Tsuji, M. Imaki, N. Kotake, A. Hirai, M. Nakaji, and S. Kameyama, "Range imaging pulsed laser sensor with two-dimensional scanning of transmitted beam and scanless receiver using high-aspect avalanche photodiode array for eye-safe wavelength," *Opt. Eng.*, vol. 56, no. 3, Nov. 2016, Art. no. 031216.

[12] A. Iizuka, S.-H. Choe, J. Hashizume, Y. Itou, and R. Okada, "Development of two-axis electromagnetic driving MEMS mirror," *Electron. Commun. Jpn.*, vol. 94, no. 11, pp. 18–23, Nov. 2011.

[13] K. Ikegami, T. Koyama, T. Saito, Y. Yasuda, and H. Toshiyoshi, "A biaxial piezoelectric MEMS scanning mirror and its application to pico-projectors," in *Proc. Int. Conf. Opt. MEMS Nanophoton.*, Aug. 2014, pp. 95–96.

[14] K. Ito, C. Niclass, I. Aoyagi, H. Matsubara, M. Soga, S. Kato, M. Maeda, and M. Kagami, "System design and performance characterization of a MEMS-based laser scanning Time-of-Flight sensor based on a 256 × 64-pixel single-photon imager," *IEEE Photon. J.*, vol. 5, no. 2, Apr. 2013, Art. no. 6800114.

[15] V. Milanovic, K. Castelino, and D. T. McCormick, "Highly adaptable MEMS-based display with wide projection angle," in *Proc. IEEE 20th Int. Conf. Micro Electro Mech. Syst. (MEMS)*, Jan. 2007, pp. 143–146.

[16] J. P. Siepmann and A. Rybaltowski, "Integrable ultra-compact, high-resolution, real-time MEMS LADAR for the individual soldier," in *Proc. IEEE Mil. Commun. Conf. (MILCOM)*, vol. 5, Oct. 2005, pp. 3073–3079.

[17] J. Zhou and K. Qian, "Low-voltage wide-field-of-view lidar scanning system based on a MEMS mirror," *Appl. Opt.*, vol. 58, no. 5, pp. A283–A290, Feb. 2019.

[18] X. Lee and C. Wang, "Optical design for uniform scanning in MEMS-based 3D imaging lidar," *Appl. Opt.*, vol. 54, no. 9, pp. 2219–2223, Mar. 2015.
[19] P. F. McManamon, P. Banks, J. Beck, D. G. Fried, A. S. Huntington, and E. A. Watson, "Comparison of flash lidar detector options," *Opt. Eng.*, vol. 56, no. 3, Mar. 2017, Art. no. 031223.
[20] C. Zhang, S. Lindner, I. M. Antolovic, J. Mata Pavia, M. Wolf, and E. Charbon, "A 30-frames/s, 252 × 144 SPAD flash LiDAR with 1728 dual-clock 48.8-ps TDCs, and pixel-wise integrated histogramming," *IEEE J. Solid-State Circuits*, vol. 54, no. 4, pp. 1137–1151, Apr. 2019.
[21] S. Jo, H. J. Kong, H. Bang, J.-W. Kim, J. Kim, and S. Choi, "High resolution three-dimensional flash LIDAR system using a polarization modulating pockels cell and a micro-polarizer CCD camera," *Opt. Express*, vol. 24, no. 26, pp. A1580–A1585, Dec. 2016.
[22] N. Radwell, A. Selyem, L. Mertens, M. P. Edgar, and M. J. Padgett, "Hybrid 3D ranging and velocity tracking system combining multi-view cameras and simple LiDAR," *Sci. Rep.*, vol. 9, no. 1, p. 5241, Dec. 2019.
[23] R. Maini and H. Aggarwal, "A comprehensive review of image enhancement techniques," 2010, *arXiv:1003.4053*. [Online]. Available: http://arxiv.org/abs/1003.4053
[24] T. Arici, S. Dikbas, and Y. Altunbasak, "A histogram modification framework and its application for image contrast enhancement," *IEEE Trans. Image Process.*, vol. 18, no. 9, pp. 1921–1935, Sep. 2009.

PALLAB K. CHOUDHURY (Member, IEEE) received the B.Sc. degree in electrical and electronic engineering from the Khulna University of Engineering and Technology (KUET), Khulna, Bangladesh, in 2003, the M.S. degree in information and communication technologies from the Asian Institute of Technology, Thailand, in 2007, and the Ph.D. degree in optical communication engineering from the Integrated Research Center for Photonics Networks and Technologies (IRCPhoNET), Scuola Superiore Sant'Anna, Pisa, Italy, in 2012.

From 2012 to 2013, he was a Research Assistant with IRCPhoNET in the research group of optical system design. Since 2018, he has been working as a Postdoctoral Fellow with the LION (LiDAR and Intelligent Optical Node) Research Laboratory, jointly formed by the Chongqing University of Technology (CQUT), Chongqing, China, and the Korea Advanced Institute of Science and Technology (KAIST), Daejeon, South Korea. He is the author of more than 40 international journals and conferences. He holds one U.S. patent. His research interests include the design and development of LiDAR for autonomous vehicle, computational imaging optics, optical wireless transmission, passive optical networks, and application of multilevel modulation formats such as OFDM. He is an Associate Editor of IEEE Access.

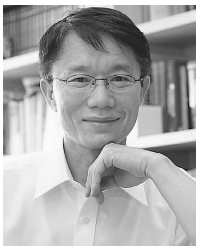

CHANG-HEE LEE (Fellow, IEEE) received the B.S. degree in electronics engineering from Hanyang University, Seoul, South Korea, in 1983, and the M.S. and Ph.D. degrees in electrical engineering from the Korea Advanced Institute of Science and Technology (KAIST), in 1985 and 1989, respectively.

From 1989 to 1990, he was a Postdoctoral Fellow with Bellcore, Red Bank, NJ, USA. From 1990 to 1997, he worked as a Senior Researcher with ETRI, Daejeon, South Korea. Since 1997, he has been a Professor with KAIST. From 2001 to 2008, he was a CTO with Novera Optics Korea Inc. From 2010 to 2011, he was the Dean of Research Affairs with KAIST. From 2013 to 2016, he was also the Head of the School of Electrical Engineering with KAIST. He is currently the Co-Dean of the LIC (Liangjiang International College) which was established by co-operation between KAIST and CQUT (Chongqing University of Technology) in China. He is the author of more than 250 international journal and conference papers. He is also an inventor of 35 patents issued in the U.S. He had spent over 30 years in the area of optical communications, including semiconductor lasers. His current research interests are in LiDAR, semiconductor lasers, optical access networks, and optical wireless communications. He is a member of OSA. He received the Haerim Photonics Technology Award, in 2013. He was granted as a top-level Foreign Talent in 2017 by the Chinese Central Government.